MOLECULAR AND CELLULAR BIOLOGY, Nov. 2005, p. 9793–9805 Vol. 25, No. 22
0270-7306/05/$08.00+0 doi:10.1128/MCB.25.22.9793–9805.2005

Mixed-Disulfide Folding Intermediates between Thyroglobulin and Endoplasmic Reticulum Resident Oxidoreductases ERp57 and Protein Disulfide Isomerase

Bruno Di Jeso,[1] Young-nam Park,[2] Luca Ulianich,[3] A. Sonia Treglia,[1] Malene L. Urbanas,[4] Stephen High,[4] and Peter Arvan[2]*

Laboratorio di Patologia Generale, Dipartimento di Scienze e Tecnologie Biologiche ed Ambientali, Facoltà di Scienze MFN, Università degli Studi di Lecce, Centro Ecotekne, 73100 Lecce, Italy[1]; Istituto di Endocrinologia ed Oncologia Sperimentale del C.N.R. "G. Salvatore" e Dipartimento di Biologia e Patologia Cellulare e Molecolare, Facoltà di Medicina e Chirurgia, Università degli Studi di Napoli "Federico II," Napoli, Italy[3]; Faculty of Life Sciences, University of Manchester, Smith Building, Oxford Road, Manchester M13 9PT, United Kingdom[4]; and Division of Metabolism, Endocrinology, and Diabetes, University of Michigan, 1500 W. Medical Ctr. Dr., Ann Arbor, Michigan 48109[2]

Received 19 February 2005/Returned for modification 2 May 2005/Accepted 29 August 2005

We present the first identification of transient folding intermediates of endogenous thyroglobulin (Tg; a large homodimeric secretory glycoprotein of thyrocytes), which include mixed disulfides with endogenous oxidoreductases servicing Tg folding needs. Formation of disulfide-linked Tg adducts with endoplasmic reticulum (ER) oxidoreductases begins cotranslationally. Inhibition of ER glucosidase activity blocked formation of a subgroup of Tg adducts containing ERp57 while causing increased Tg adduct formation with protein disulfide isomerase (PDI), delayed adduct resolution, perturbed oxidative folding of Tg monomers, impaired Tg dimerization, increased Tg association with BiP/GRP78 and GRP94, activation of the unfolded protein response, increased ER-associated degradation of a subpopulation of Tg, partial Tg escape from ER quality control with increased secretion of free monomers, and decreased overall Tg secretion. These data point towards mixed disulfides with the ERp57 oxidoreductase in conjunction with calreticulin/calnexin chaperones acting as normal early Tg folding intermediates that can be "substituted" by PDI adducts only at the expense of lower folding efficiency with resultant ER stress.

Membrane and secretory proteins are cotranslationally translocated in the lumen of the endoplasmic reticulum (ER), where they acquire their three-dimensional structure (including the formation and isomerization of disulfide bonds), typically culminating in oligomeric assembly. This is a complex task, both facilitated and monitored by ER folding enzymes and molecular chaperones. Glycoproteins are an important subset of exportable proteins, and those bearing Asn-linked oligosaccharides fold preferentially with the aid of calreticulin (CRT) and calnexin (CNX), both of which possess a lectin-like binding site that prefers association with monoglucosylated oligosaccharide processing intermediates (4). CRT and CNX might directly influence protein folding (32), but an additional critical function of these proteins is to bring newly synthesized exportable glycoproteins in close proximity with ERp57 (47), an oxidoreductase that works in a complex with CRT/CNX and promotes proper disulfide bond formation (21, 46, 54).

Another molecular chaperone is BiP (GRP78), which binds to unfolded polypeptides, helps to prevent protein aggregation through noncovalent associations regulated by its ATPase domain (9), and works cooperatively with protein disulfide isomerase (PDI) to promote oxidative protein folding (36). Indeed, recently the concept of two distinct chaperone-oxidoreductase complexes, one comprising CRT/CNX/ERp57 and the other including BiP/PDI (37), has emerged. This fits well with earlier proposals of a reticular-like matrix in the ER lumen in which different chaperone systems are organized (25, 51). In this view, PDI plays a role in the BiP system analogous to that of ERp57 in the CRT/CNX system. However, while the absence of the CRT contribution to the ERp57 system can be functionally compensated for by the presence of CNX, the simultaneous absence of both lectin-like chaperones cannot be compensated for by BiP (40).

In vitro studies suggest that mixed-disulfide bonds between oxidoreductase and substrate polypeptides are intermediates in the formation of native intrachain disulfide bonds (23). Such mixed disulfides have been described for virally infected cells (42) and for cells overexpressing various exportable proteins after transfection (1–3, 38). Lindquist et al. (34) have even reported a mixed disulfide between ERp57 and newly synthesized endogenous major histocompatibility complex class I molecules, but it has remained unclear whether the intermolecular association recovered represents an authentic, covalent oxidoreductase-unfolded substrate intermediate (10). Thus, the challenge to isolate mixed disulfides between endogenous oxidoreductases and endogenous unfolded substrates (17) has yet to be convincingly achieved.

Native thyroglobulin (Tg), the precursor protein for thyroid hormone synthesis, is a large secretory glycoprotein comprised of noncovalently associated homodimers of 660 kDa (28), with up to 60 intramolecular disulfide bonds and 10 to 15 N-linked oligosaccharides per Tg monomer (11). The folding of newly synthesized Tg is slow: completion of oxidative folding requires

* Corresponding author. Mailing address: Division of Metabolism, Endocrinology, & Diabetes, University of Michigan, 1150 W. Medical Ctr. Dr., Ann Arbor, MI 48109. Phone: (734) 936-5505. Fax: (734) 936-6684. E-mail: parvan@umich.edu.

about 60 to 90 min (14), while the half-life of medial Golgi arrival is about 90 to 120 min (29). Multiple ER resident proteins, including CRT/CNX (14) and BiP (26, 27), have been implicated in Tg folding. In this report we wished to test the hypothesis that in living cells, the folding pathway of Tg, as a representative exportable glycoprotein, is likely to involve distinct chaperone-oxidoreductase systems that include formation of distinct mixed-disulfide complexes. As the dominant glycoprotein synthesized endogenously in thyrocytes, Tg presents itself as a unique model protein with which to explore this hypothesis.

MATERIALS AND METHODS

Materials. Coon's modified Ham's F-12 medium was from Sigma. Protein A-Sepharose was from Calbiochem. Endo-β-*N*-acetylglucosaminidase H (endo H) was from Roche. Peptide *N*-glycohydrolase F (PNGase F) was from New England Biolabs. [^{35}S]cysteine and [^{35}S]methionine Promix was from Amersham. Polyvinylidene difluoride membranes were from Millipore. The enhanced chemiluminescence kit was from Amersham. All other chemicals were from Sigma.

Cell culture and biological reagents. FRTL-5 (ATCC CRL 8305) (F. S. Ambesi-Impiombato, 1986, U.S. patent no. 4,608,341) and PC-Cl3 cells are continuous, cloned lines of thyroid differentiated cells. These cells were maintained as described previously (12). Polyclonal anti-Tg rabbit antibodies were raised against rat Tg as previously described (12). Anti-CNX antibodies were from Stressgen; anti-CRT, anti-BiP, and anti-GRP94 antibodies were from Affinity Bioreagents; and anti-IκB antibodies were from Santa Cruz Biotechnology.

Metabolic labeling and immunoprecipitation. FRTL-5 and PC-Cl3 cells were incubated for 30 min in methionine-free, cysteine-free medium, labeled for 15 min (unless otherwise indicated) at 37°C in the same medium containing 50 μCi/ml [^{35}S]cysteine and [^{35}S]methionine labeling mix, and chased either in complete medium with an excess of cold methionine and cysteine or, for experiments employing thapsigargin, in a nominally free Ca^{2+} medium with the same excess of unlabeled amino acids. All subsequent manipulations were performed at 4°C. The labeled cells were washed with cold phosphate-buffered saline (PBS) containing 20 mM *N*-ethylmaleimide (NEM) in order to alkylate free sulfhydryls and lysed in 1 ml of lysis buffer (150 mM NaCl, 0.5% Triton X-100, 25 mM Tris [pH 7.4], and Complete protease inhibitor mixture [Roche]) plus 20 mM NEM. Nuclei and cell debris were removed by centrifugation at 10,000 × *g* for 10 min at 4°C. The lysates were incubated for 1 h at 4°C with the respective antibodies and tumbled with protein A-Sepharose for 3 h. The beads were washed three times with lysis buffer and boiled in sodium dodecyl sulfate (SDS) sample buffer (4% SDS, 0.2% bromophenol blue, 20% glycerol, 100 mM Tris-HCl [pH 6.8]) with or without 20 mM dithiothreitol, and the supernatant was subjected to SDS-polyacrylamide gel electrophoresis (SDS-PAGE) and autoradiography.

For BiP immunoprecipitation, labeled cells were washed with cold PBS containing 20 mM NEM and then three times with PBS alone and lysed in 1 ml of lysis buffer plus 20 U/ml apyrase (to enzymatically deplete ATP). After 60 min, cells were processed as described above.

For immunoprecipitations of GRP94 and BiP, in situ chemical cross-linking was performed as previously reported (43), with minor modifications. Briefly, labeled cells were rinsed with PBS and then incubated at 4°C for 30 min with 2 mM dithiobis(succinimidylpropionate) (DSP) freshly prepared in 90% PBS, 10% dimethyl sulfoxide. Control samples were incubated identically but without DSP. Cells were then rinsed with cold PBS and alkylated with 20 mM NEM. Cells were lysed with 1 ml of lysis buffer plus 20 mM NEM and 50 mM glycine to quench excess cross-linker. Lysates were then processed as described above.

For immunoprecipitation in denaturing conditions, cells were labeled, washed, and lysed as described above. One-half of the lysate was immunoprecipitated as described above, and the other half was brought to 5% SDS and boiled for 5 min. The latter samples were then diluted 10-fold with 1% Triton X-100 in 150 mM NaCl, 25 mM Tris (pH 7.4). Immunoprecipitates of denatured samples were washed three times with 0.05% Triton X-100, 0.1% SDS, 0.3 M NaCl, 10 mM Tris (pH 8.6). For some experiments (see Fig. 4C and D and 5), the amount of lysate immunoprecipitated with anti-ERp57 and anti-PDI and their respective controls was three times greater than the amount of lysate immunoprecipitated with anti-Tg, in order to obtain comparable band intensities and to accurately judge band migration. For sequential immunoprecipitation, the samples were first immunoprecipitated under nondenaturing conditions and then brought to 5% SDS and boiled for 5 min. The samples were then diluted 10-fold with 1% Triton X-100, 150 mM NaCl, 25 mM Tris (pH 7.4) and reimmunoprecipitated. Quantitations were performed using a PhosphorImager from Molecular Dynamics.

Western blotting. PC-Cl3 cells were pretreated for 1 h with 6 μg/ml cycloheximide, followed by 0.5 ng/ml tumor necrosis factor (TNF) for 60 and 180 min. Alternatively, cells were pretreated for 1 h with 6 μg/ml cycloheximide plus in the last 10 min with 10 μM MG132, followed by 0.5 ng/ml TNF for 60 and 180 min. After evaluation of protein content, 30 μg of cell extract was analyzed by SDS-PAGE and electrotransferred to polyvinylidene difluoride. Blocking was for 15 h at 4°C with Tris-buffered saline–Tween 20 (TBST) buffer (10 mM Tris [pH 8.0], 150 mM NaCl, 0.1% Tween 20) containing 10% nonfat dry milk, followed by incubation in TBST buffer for 2 h at room temperature with a 1:2,000 dilution of anti-IκB. After being washed with TBST, the blot was incubated for 1 h at room temperature with antirabbit horseradish peroxidase-conjugated antibodies diluted 1:3,000 in TBST. Band detection was by enhanced chemiluminescence.

In vitro transcription/translation of truncated Tg. The coding region from the rat Tg cDNA was excised from the rTg-2 plasmid in pCDNA3 (19) with EcoRI and HincII and subcloned into the EcoRI and SmaI sites of pGEM7z. A DNA template encoding the rat Tg signal peptide plus the first 177 residues of the mature rat protein and lacking a stop codon was generated by linearizing the DNA with HindIII. This was transcribed with T7 RNA polymerase (Promega), and the resulting mRNA was translated in a rabbit reticulocyte lysate system supplemented with canine pancreatic microsomes and [^{35}S]methionine (47) for 25 min at 30°C. When protein synthesis was followed by treatment with puromycin (2 mM), a synthesis period of 15 min at 30°C was followed by a further 15 min at 30°C with puromycin to force release of nascent rat Tg chains from the ribosome (47). When employed, castanospermine (CST) was included in the translation mix at 1 mM. After synthesis and puromycin treatment as appropriate, membrane-associated chains were isolated by centrifugation, resuspended, and analyzed directly or following treatment with 50 μM bismaleimidohexane, a homobifunctional alkylating agent that reacts with free cysteine residues (15). Total products were recovered by precipitation with trichloroacetic acid and then solubilization in SDS sample buffer, whereas specific products recovered by immunoprecipitation with antisera specific for Tg, ERp57, and PDI were treated as previously described (15). The labeled proteins were finally analyzed by SDS-12% PAGE under reducing conditions.

Other procedures. Sucrose gradient centrifugation, endo H, and PNGase F digestions were performed as reported previously (12, 13).

RESULTS

Intermolecular disulfide-linked adducts containing newly synthesized Tg in the folding pathway. In the absence of chemical cross-linkers, newly synthesized Tg immunoprecipitated from PC-Cl3 or FRTL-5 cells was resolved as multiple species upon nonreducing SDS-PAGE. The most abundant species had a molecular mass of 330 kDa (the size of "free" monomers) (Fig. 1A), which migrated slightly faster than the intracellular Golgi form (termed band "G") that serves as the immediate precursor to Tg recovered in culture media (Fig. 1A). At early chase times, three higher-molecular-mass species, termed bands "A," "B," and "C" were also specifically immunoprecipitated with anti-Tg antibodies (band B may be comprised of two subcomponents; see below). Although precise high-molecular-mass markers are unavailable, we estimate that bands A, B, and C migrated approximately in the 390- to 480-kDa region of the gel, much more slowly than secreted Tg or Tg with fully reduced thiols (Fig. 1A, left), indicating that these bands could not possibly represent partially oxidized free Tg monomers. Indeed, under reducing conditions, Tg species A, B, and C were no longer recovered, suggesting that they represent covalent adducts of newly synthesized Tg interacting via mixed disulfides with one or more proteins (Fig. 1A, right). These adducts were more readily detected at early chase times. Interestingly, the time-dependent disappearance of these minor Tg species in cells correlated well with the kinetics of Tg dissociation from CRT and CNX (as quantified by Tg coim-

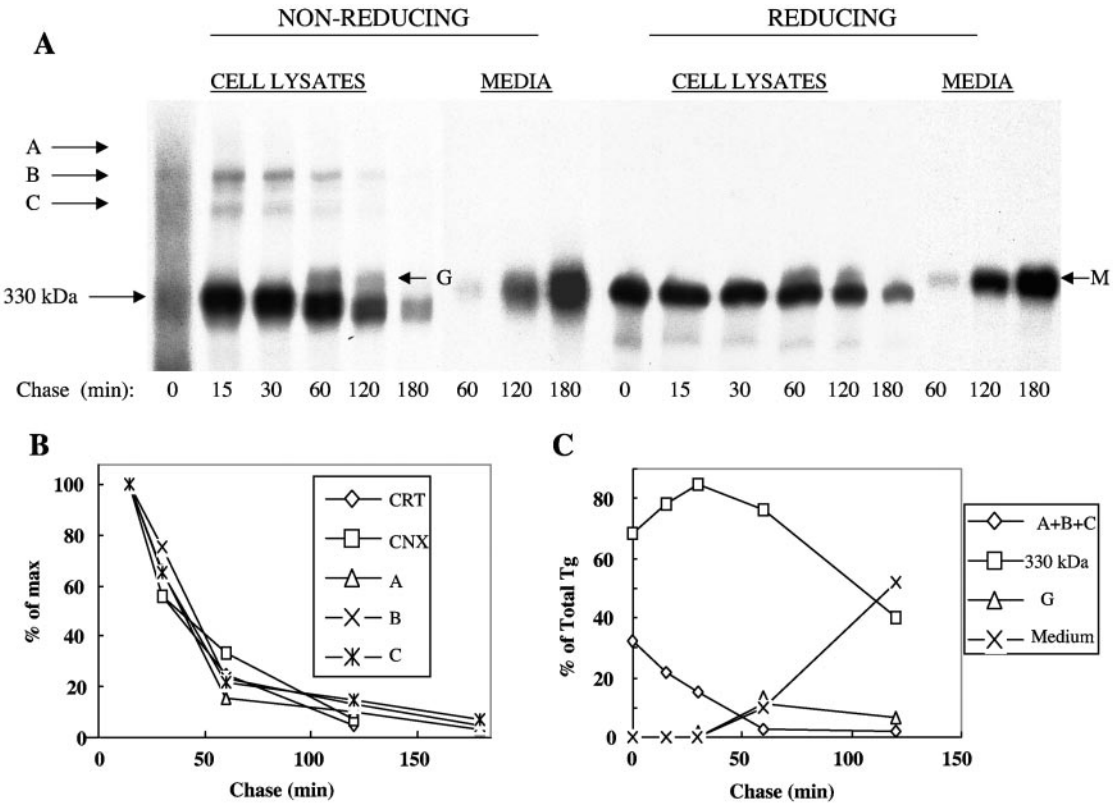

FIG. 1. During folding, Tg forms intermolecular disulfide-bonded complexes. (A) PC-Cl3 cells were labeled as outlined in Materials and Methods and chased for the indicated times. Cell lysates and culture media were immunoprecipitated with anti-Tg antibodies. Immunoprecipitates were resolved by SDS-PAGE under nonreducing and reducing conditions. The positions of Tg secreted to the medium (M), 330-kDa Tg, Golgi Tg (G), and intermolecular disulfide-linked adducts (A, B, and C) are indicated. The gels were intentionally overexposed in order to optimally visualize the presence of bands A, B, and C under nonreducing conditions and their absence under reducing conditions. For densitometry, shorter exposures were used. (B) Kinetics of band A, B, and C disappearance as well as Tg coimmunoprecipitation with CRT and CNX. The means of three separate experiments have been plotted. max, maximum. (C) Kinetics of recovery for each of the various forms of Tg. The term "330 kDa" refers to Tg recovered intracellularly at the 330-kDa position as indicated in panel A. The mean values from three separate experiments have been plotted.

munoprecipitation [Fig. 1B]). When Tg was immunoprecipitated immediately after a short pulse (30 s; data not shown), it was already possible to isolate disulfide-linked Tg complexes, indicating that adduct formation begins as an early event in Tg folding. Not surprisingly, disulfide-linked Tg complexes were completely endo H sensitive (Fig. 2A).

Importantly, despite being adducts, Tg species A, B, and C were recovered within the broad sucrose gradient peak comprising Tg monomers and not at all recovered in the Tg dimer fraction (Fig. 2B), thereby excluding the possibility that these species represent improperly formed homotypic covalent complexes (i.e., between Tg and other copies of itself).

Next, we asked if these disulfide-linked Tg adducts might be normal Tg folding intermediates en route to secretion. Three lines of reasoning support the conclusion that species A, B, and C are unlikely to be "dead-end" products destined for ER-associated degradation (ERAD). First, Tg A, B, and C band intensities were maximal immediately after the pulse and declined thereafter (Fig. 1A and B), whereas "dead-end" ER folding byproducts are generally reported to accumulate after a lag before their proteasomal degradation (6, 7). Indeed, both short pulse-labeling studies and in vitro translation studies (described below) suggest that formation of disulfide-linked Tg adducts may occur even before nascent Tg molecules have completed their translation/translocation into the ER, prior to any commitment of the polypeptide to "on-pathway" or "off-pathway" products. Second, quantitation of the abundance of intermolecular disulfide-bonded Tg species showed that the initially recovered amount was nearly 30% of total Tg, while time-dependent disappearance of these species was not accompanied by any loss of total Tg (total being the sum of all species shown in Fig. 1C), consistent with the interconversion of Tg forms rather than ERAD.

Finally, we tested directly the disappearance of the species A, B, and C in the presence of 10 μM MG132, an inhibitor of the 26S proteasome. As a control, we confirmed that this dose of MG132 quantitatively blocked TNF-induced proteasomal degradation of IκB (8) in the same cells over a 4-h period (data not shown). Although proteasome inhibition slowed the secretory process for newly synthesized Tg from cells to medium, the disappearance of Tg adducts was not blocked (Fig. 3, top; kinetics shown at bottom right). Kifunensine, the ER mannosidase I inhibitor, is also exceptionally effective in blocking the ERAD of misfolded Tg species (52); nevertheless, this too

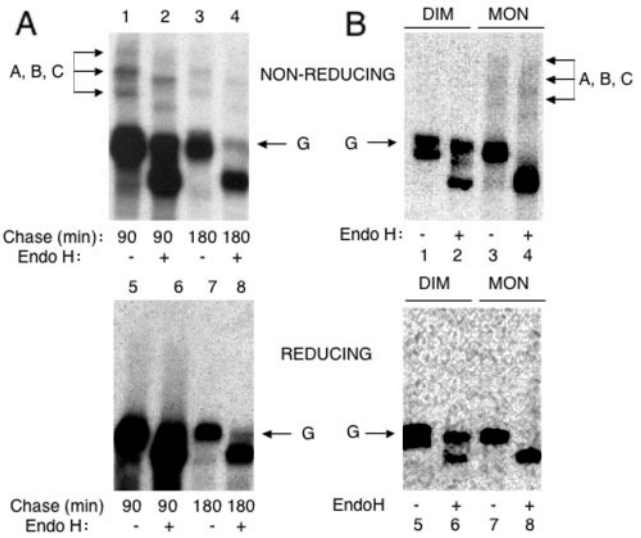

FIG. 2. Intermolecular disulfide-linked Tg adducts are endo H sensitive and cosediment with monomeric Tg. (A) PC-Cl3 cells were labeled as outlined in Materials and Methods and chased for the indicated times. Cell lysates were immunoprecipitated with anti-Tg antibodies and digested or mock digested with endo H. (B) PC-Cl3 cells were labeled as outlined in Materials and Methods and chased for 90 min. Cell lysates were subjected to sucrose gradient centrifugation, and selected fractions from the dimer (DIM) and monomer (MON) peaks were immunoprecipitated with anti-Tg antibodies and mock-digested or digested with endo H. For both panels, immunoprecipitates were resolved by SDS-PAGE under nonreducing (lanes 1 to 4) and reducing (lanes 5 to 8) conditions. The positions of Golgi Tg (G) and intermolecular disulfide-bonded Tg complexes (A, B, and C) are indicated.

failed to prevent disappearance of Tg adducts (Fig. 3, top). Although the data do not formally exclude the possibility of ERAD for some subpopulation of disulfide-linked Tg complexes, taken together, the results are consistent with the hypothesis that species A, B, and C are disulfide-linked adducts that involve endogenous newly synthesized Tg en route to productive folding.

Higher-molecular-mass Tg complexes include noncovalent chaperone associations as well as covalent, disulfide-linked ERp57- and PDI-containing adducts. Because many ER resident proteins are long-lived, to begin to explore the protein composition of higher-molecular-mass Tg complexes, we radiolabeled thyrocytes with ^{35}S-amino acids for 48 h in the hopes of identifying slowly labeled ER resident oxidoreductases that might form disulfide-linked adducts with newly synthesized, immunoprecipitated Tg. After resolution by SDS-PAGE and exposure to X-ray film, the region containing disulfide-linked adducts A, B, and C was identified, excised, and reanalyzed by SDS-PAGE under reducing conditions (Fig. 4A). As expected, labeled 330-kDa Tg was the major radioactive component from these reanalyzed Tg immunoprecipitates. At least three additional protein bands were also recovered in the molecular mass region between 49.5 kDa and 80 kDa, which might plausibly include PDI, ERp57, and ERp72, as well as other ER resident proteins. To begin to identify some of the specific components of the high-molecular-mass Tg complexes, we then performed a series of immunoprecipitation experiments.

Under nondenaturing conditions, immunoprecipitations of CRT and CNX are known to coimmunoprecipitate Tg (Fig. 1B; see also reference 14). When such immunoprecipitates were analyzed by nonreducing SDS-PAGE, antibodies to CRT and CNX coimmunoprecipitated disulfide-linked Tg adducts A, B, and C (Fig. 4B, left). CRT coprecipitated more Tg than did CNX and concomitantly coprecipitated more Tg adducts. However, under denaturing conditions, anti-CRT and anti-CNX antibodies could no longer coimmunoprecipitate Tg adducts (Fig. 4B, right), indicating that CRT and CNX were not directly involved in mixed disulfides with Tg.

Cell lysates were then immunoprecipitated under nondenaturing and denaturing conditions with anti-ERp57 and anti-PDI. Both antibodies immunoprecipitated disulfide-linked Tg adducts under nondenaturing conditions (Fig. 4C, left), as expected. Also, dramatically, under denaturing conditions, anti-ERp57 and anti-PDI effectively coimmunoprecipitated newly synthesized disulfide-linked Tg adducts (Fig. 4C, right), suggesting that these oxidoreductases were directly covalently bound to Tg. In particular, ERp57 appeared to be engaged primarily with a slower subcomponent of the B species, while PDI appeared to be engaged primarily with a faster subcomponent (Fig. 4C). By contrast, only a negligible fraction of 330-kDa monomeric Tg was coimmunoprecipitated with anti-ERp57 or anti-PDI antibodies even under nondenaturing conditions, indicating that most of the recoverable Tg interactions with these oxidoreductases employ mixed-disulfide bonds.

To directly demonstrate that disulfide-linked Tg adducts contain ERp57 and PDI, we performed sequential immunoprecipitation experiments. Tg immunoprecipitates were again denatured before a second-round immunoprecipitation was performed; anti-ERp57 still specifically recovered the major, slower B subcomponent of Tg, while anti-PDI still specifically recovered the minor, faster B subcomponent (Fig. 4D). Under reducing conditions, the complexes dissociated and the Tg contained in both ERp57- and PDI-containing adducts ran with identical mobility (and increased intensity) at the 330-kDa monomer position.

As PDI and ERp57 differ in molecular mass by only a few kilodaltons, this alone would not be expected to be distinguishable by SDS-PAGE in the 400-kDa molecular mass region. (Preliminary time course experiments established that our incubation conditions gave complete PNGase F digestion.) We considered that these distinct Tg adducts might reflect sequential complexes in the Tg folding pathway, with progression of intramolecular Tg oxidation to the faster migrating subcomponent. If sequential, then one might expect a significant time-dependent shift of Tg from one chaperone-oxidoreductase complex to another. However, when the relative recovery of labeled Tg engaged in mixed disulfides with ERp57 and PDI was compared by coimmunoprecipitation from pulse-labeled thyrocytes at 10 min versus 60 min of chase, there was little shift in the relative distribution of labeled Tg from one covalent complex to the other (Fig. 5, left). This experiment was then repeated in cells pretreated with the glucosidase inhibitor CST, which blocks the lectin-like binding of CRT/CNX to nascent Tg (14). Under these conditions, formation of Tg-ERp57 adducts was abrogated, while recovery of Tg-PDI ad-

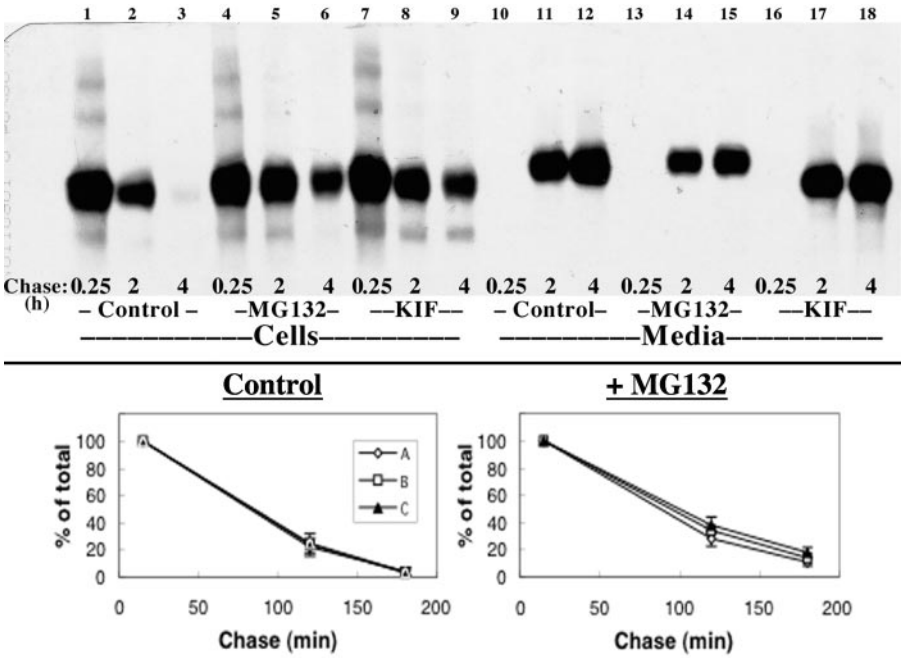

FIG. 3. The A, B, and C species represent intermediates of the productive folding pathway of Tg. (Top) PC-Cl3 cells were labeled as outlined in Materials and Methods and chased for up to 4 h in the absence or presence (during labeling and chase) of 10 μM MG132 or 100 μM kifunensine (KIF). Cell lysates (lanes 1 to 9) and culture media (lanes 10 to 18) were immunoprecipitated with anti-Tg antibodies. Immunoprecipitates were resolved by nonreducing SDS-PAGE. The intermolecular disulfide-bonded Tg complexes (A, B, and C) are clearly visible at time zero but subsequently disappear. (Bottom) Time course of the disappearance of the species A, B, and C in the absence or presence of 10 μM MG132. Each value shown is the mean from three experiments.

ducts was not diminished (and actually appeared to increase) (Fig. 5, right).

Since it has been estimated to require several minutes to translate the entire Tg polypeptide (11), we sought evidence that initial Tg interaction with ERp57 and PDI might occur even before completion of nascent chain synthesis. We therefore exploited a truncated N-terminal Tg fragment encoding the first, amino-terminal Asn-linked glycosylation site (at residue 91 of the mature polypeptide) and including 15 Cys residues as potential targets for the thiol-specific cross-linking analysis previously used to identify the interaction of ERp57 with newly synthesized glycoproteins (47). When mRNA was omitted from the otherwise complete in vitro translation reaction, no labeled peptides were detected (data not shown). However, when the Tg fragment was synthesized as a ribosome-bound translocation intermediate in the presence of dog pancreas microsomes, labeled truncated Tg chains in the ~25-kDa range were produced and these appeared endo H sensitive (Fig. 6A), confirming that the N-terminal region of the truncated polypeptide had been translocated into the ER lumen and modified by N glycosylation. When the translocation intermediates were treated with puromycin (forcing release from ribosomes), association of the Tg fragment with ER luminal chaperones could be stabilized by cross-linking, and under normal conditions, discrete adducts with both ERp57 and PDI could be observed after immunoprecipitation (Fig. 6B, lanes 3 and 4). (Since truncated rat Tg is in the 20- to 30-kDa range and ERp57 is ~57 kDa, a 1:1 cross-link stoichiometry should produce adduct bands that run in the 80- to 90-kDa range if molecular mass is taken as the only consideration.) Anti-ERp57 selectively pulled down two cross-linked Tg adducts of about 130 kDa and 80 kDa, while anti-PDI pulled down (more weakly) two cross-linked Tg adduct bands that were faster in mobility than their ERp57-Tg counterparts. When a similar analysis was carried out with CST present during translation to prevent the trimming of glucose residues from the N-glycan present on the Tg fragment, the association between ERp57 and the truncated Tg could no longer be detected. These data indicate that the cross-linking to ERp57 observed under control conditions reflects specific interactions. Under conditions of CST treatment, both Tg translation efficiency and association between PDI and truncated Tg were unaffected (Fig. 6B). Taken together, these data suggest that the N-terminal fragment of Tg has sufficient information to recruit the ER oxidoreductases ERp57 and PDI, with the association of ERp57 being dependent upon the presence of a correctly trimmed N-linked glycan.

CST decreases efficiency of Tg folding. Prevention of both CNX/CRT interaction and ERp57 adduct formation for newly synthesized Tg in cells pretreated with CST provides an opportunity to examine the significance of the contribution of ERp57 oxidoreductase activity in Tg maturation and to review earlier conclusions suggesting that ER glucosidase inhibition has only very limited effects on Tg secretion (16). Under CST pretreatment conditions (which shift nascent Tg folding complexes away from ERp57 adducts but not away from PDI adducts [Fig. 5]), the disappearance of Tg adducts appeared delayed (Fig. 7, top; quantitated in line drawing, bottom). Tg

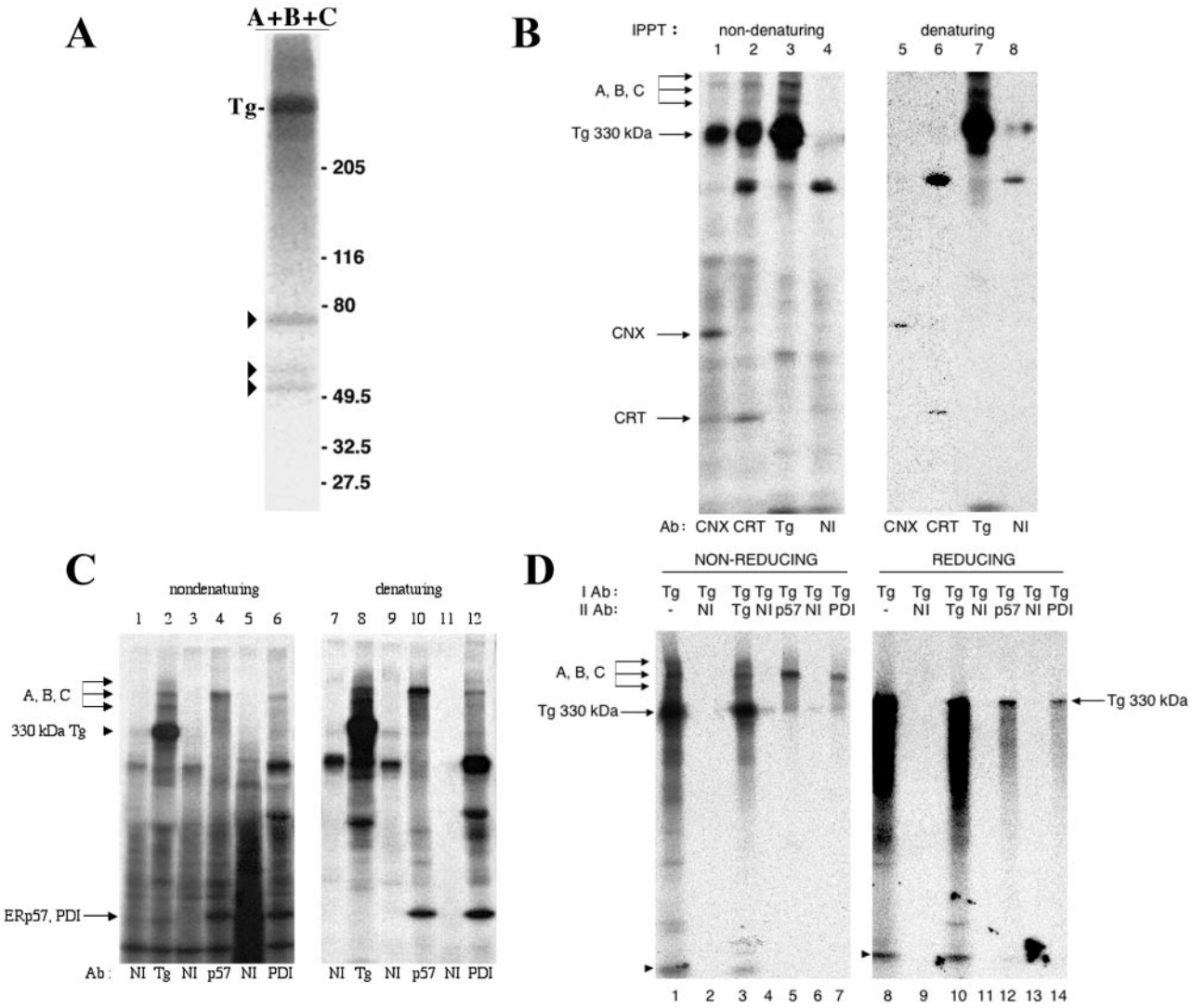

FIG. 4. High-molecular-mass Tg complexes include noncovalently associated chaperones as well as adducts involving ERp57-Tg and PDI-Tg mixed disulfides. (A) PC-Cl3 cells were metabolically labeled continuously for 48 h. Immunoprecipitated Tg was analyzed by nonreducing SDS-PAGE. The radioactive sample was exposed to film and realigned with the original sample, and the disulfide-linked Tg adducts A, B, and C were excised, eluted, and reanalyzed by SDS-PAGE under reducing conditions. Associated bands liberated upon reduction of Tg adducts are highlighted with arrowheads; the positions of molecular mass markers (in kiladaltons) are shown at right. (B) CRT and CNX associate noncovalently with bands A, B, and C. PC-Cl3 cells were labeled as outlined in Materials and Methods and chased for 15 min. Cell lysates were immunoprecipitated (IPPT) under nondenaturing or denaturing conditions with nonimmune serum (NI) or anti-Tg, anti-CRT, or anti-CNX antibody (Ab) and resolved by nonreducing SDS-PAGE. The positions of the 330-kDa Tg, intermolecular disulfide-linked Tg adducts (A, B, and C), CRT, and CNX are indicated. (C) Immunoprecipitation of ERp57 and PDI recovers Tg adducts representing mainly the B species. PC-Cl3 cells were labeled and chased as described for panel B. Cell lysates were immunoprecipitated under nondenaturing and denaturing conditions with nonimmune serum or anti-Tg, anti-ERp57, anti-EsR (a negative control), or anti-PDI antibody and resolved by nonreducing SDS-PAGE. The positions of the 330-kDa Tg, intermolecular disulfide-linked Tg adducts (A, B, and C), ERp57, and PDI are indicated. (D) Direct proof that ERp57 and PDI are engaged in mixed disulfides with Tg. PC-Cl3 cells were labeled and chased as described for panel B. Cell lysates were first immunoprecipitated with anti-Tg antibodies and then boiled in SDS and finally reimmunoprecipitated with nonimmune serum or anti-Tg, anti-ERp57, anti-EsR (a negative control), or anti-PDI antibody and resolved by nonreducing and reducing SDS-PAGE. The positions of the 330-kDa Tg and intermolecular disulfide-linked Tg adducts (A, B, and C) are indicated. Retardation of a low-molecular-mass protein (near bottom of the gel) is indicative of reduction of proteins in the gel.

secretion was also decreased, and by SDS-PAGE the main secreted Tg band migrated distinctly from normal (consistent with persistence of terminal glucoses on N-glycans). In addition, there was a "streak" of Tg molecules which migrated above the main Tg band and which was still apparent under reducing conditions (Fig. 7; discussed further below). The distinct mobility of newly synthesized Tg after CST pretreatment could reflect differences in either carbohydrate processing or folding, or both. Certainly, after CST pretreatment, carbohydrate processing was altered such that Tg never acquired endo H resistance, regardless of folding, dimerization, or secretion (Fig. 8A). However, to evaluate Tg disulfide maturation inde-

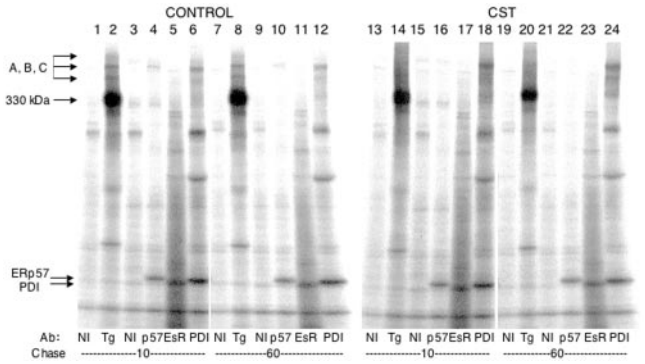

FIG. 5. ERp57 operates early in the folding pathway of Tg and in a CRT/CNX-dependent manner, while PDI action is more extended in time and is not dependent on CRT/CNX. PC-Cl3 cells were pretreated or not with CST and then labeled as outlined in Materials and Methods and chased for 10 and 60 min in the presence or absence of CST. Cell lysates were immunoprecipitated under nondenaturing conditions with nonimmune serum (NI) or anti-Tg, anti-ERp57, anti-EsR (a negative control), or anti-PDI antibody (Ab) and resolved by nonreducing SDS-PAGE. The positions of the 330-kDa Tg, intermolecular disulfide-bonded complexes (A, B, and C), ERp57, and PDI are indicated.

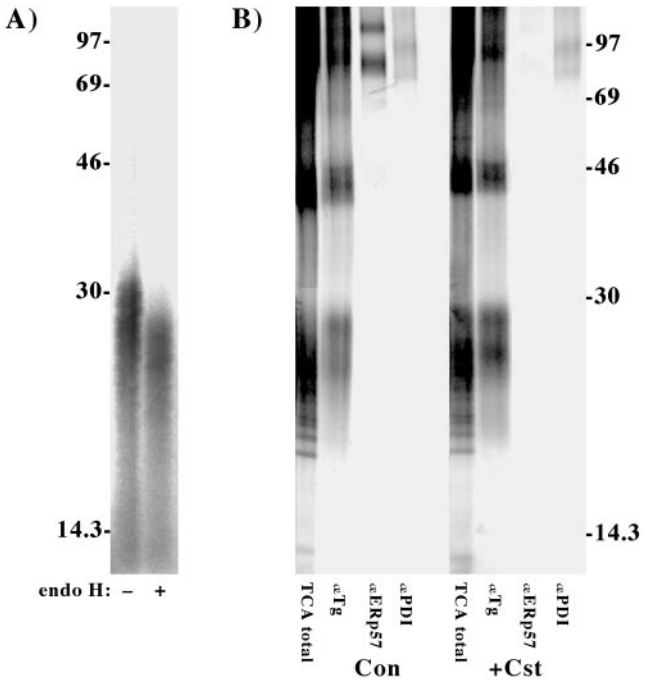

FIG. 6. Translation of truncated Tg bearing only the first N-glycosylation site, and association of the truncated protein with ERp57 and PDI. A cDNA encoding a truncated rat Tg lacking a stop codon was prepared as outlined in Materials and Methods. Using a coupled in vitro transcription/translation system, the truncated protein was synthesized in the presence of ^{35}S-amino acids and pancreatic microsomes. (A) The translation period was 25 min and was concluded without the use of puromycin. The labeled products were analyzed by SDS-PAGE after mock-digestion or digestion with endo H. (B) The in vitro translation either omitted (control [Con]) or included (+Cst) 1 mM CST, and all translations were terminated by incubation with 2 mM puromycin to release nascent chains. The translation mix was divided into four equal portions that were either precipitated with 10% trichloroacetic acid (TCA) or immunoprecipitated with one of the antibodies shown. Molecular mass markers (in kilodaltons) are shown at sides of gels.

pendently of the consideration of differences in glycosylation, samples were first treated with PNGase F. Importantly, deglycosylated Tg derived from CST-treated cells showed an abnormally slow SDS-PAGE mobility selectively under nonreduced (but not reduced) conditions (Fig. 8B). Together the data suggest that concomitant with loss of formation of ERp57-containing adducts is a folding defect of newly synthesized Tg, including impairment/delay of adduct resolution and intrachain disulfide bond maturation (Fig. 7 and 8B), which is essential to the dimerization that leads to Tg secretion (14).

Quality control of Tg in the ER of thyrocytes after CST pretreatment. To further explore the secretory defect after CST pretreatment, we examined Tg dimerization by sedimentation velocity sucrose gradient centrifugation. We found that efficiency of Tg dimerization was significantly diminished, as reflected by an increased monomer:dimer ratio (Fig. 8C). Under the expected conditions of normal ER quality control, an increased load of undimerized Tg is predicted to be efficiently retained within the ER and prevented from anterograde transport until the impaired/delayed maturation of intrachain disulfide bonds has been rectified or the molecules degraded by ERAD. Our observations partially fulfilled these predictions.

On one hand, quantitation of total labeled Tg at 120 and 180 min of chase indicated diminished recovery (30 and 40%, respectively) in CST-pretreated cells (Fig. 8D), suggesting enhanced ERAD. As noted above, ERAD of misfolded Tg is known to be inhibited by kifunensine, an inhibitor of ER mannosidase I (52) that processes ERAD substrates for retrotranslocation in conjunction with EDEM family members (22, 35, 39, 44, 45, 53). The fact that kifunensine blocked the diminished recovery of labeled Tg (Fig. 8D) strongly suggests enhanced ERAD of labeled Tg in CST-pretreated cells.

On the other hand, after CST pretreatment, labeled Tg did not appear to be efficiently retained within the ER, as a significant fraction of secreted Tg was recovered as monomers (Fig. 9A), suggesting a decrease in the quality control of Tg in the ER. While it could be argued that these "secreted monomers" are an artifact of dimer dissociation during sucrose gradient centrifugation, this is probably not the case. Clearly, deglycosylated Tg monomers recovered intracellularly from CST-pretreated cells had incomplete disulfide oxidation (a slightly slower mobility upon nonreducing SDS-PAGE) compared to those from control cells (Fig. 9B, lane 16 versus lane 15). Although subtle, most of the secreted deglycosylated Tg recovered as monomers from CST-pretreated cells (Fig. 9B, lane 8) appeared to match the band mobility of intracellular monomers from these cells (Fig. 9B, lane 16) more closely than that from intracellular dimers within the same cells (Fig. 9B, lane 12). In this case, the monomers recovered in the secretion from CST-pretreated cells must be comprised at least in part of Tg molecules secreted directly as free monomers rather than as dimers. Because proper monomer folding and efficient Tg dimerization normally occur within the ER before export (14, 26), the export of free monomers indicates diminished ER quality control of Tg after CST pretreatment in addition to the enhanced ERAD. None of these effects were mediated by any detectable change in ER chaperone levels during at least the first 2 h of these experiments (data not shown).

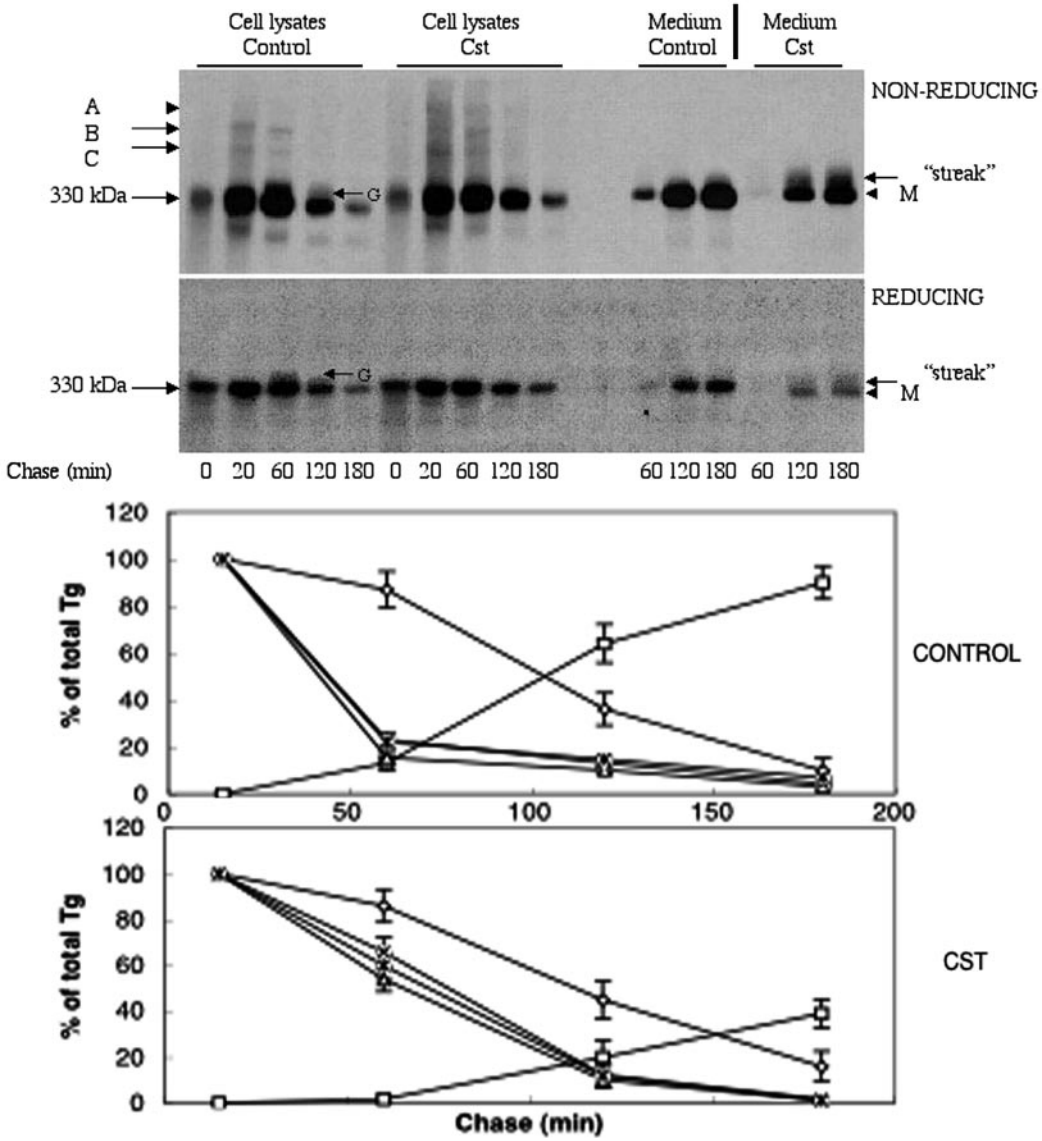

FIG. 7. CST inhibits but does not block Tg secretion and adduct maturation. PC-Cl3 cells were preincubated with 1 mM CST for 1 h and then labeled and chased in the presence of CST. Cell lysates and culture media were immunoprecipitated with anti-Tg antibodies. (Top) Immunoprecipitates were resolved by SDS-PAGE. The positions of Tg secreted to the medium (M), 330-kDa Tg, Golgi Tg (G), and intermolecular disulfide-bonded Tg complexes (A, B, and C) are indicated. The gels were intentionally overexposed in order to improve the visualization of bands A, B, and C under nonreducing conditions and to document their absence under reducing conditions. (Bottom) The disappearance of bands A, B, and C (triangles, X's, and filled squares, all overlapping) and 330-kDa Tg (circles) and the appearance of Tg in the medium (open squares) have been quantitated from the means of three experiments under control and CST pretreatment conditions, as shown.

Acutely after CST pretreatment, newly synthesized Tg binding to BiP and GRP94 was dramatically increased (Fig. 9C), a feature reminiscent of the shift of Tg chaperone preference from CRT/CNX/ERp57 to BiP and GRP94 that occurs after thapsigargin treatment (14). Indeed, after thapsigargin, an even stronger ER perturbant than CST, there is a very poor ability of thyrocytes to advance disulfide-linked Tg adducts through the folding pathway (Fig. 9D) and the *u*nfolded *p*rotein *r*esponse (UPR) is strongly activated (14, 33). Under such conditions, increased engagement of BiP with Tg (14, 30) or other proteins in the ER is typically associated with UPR activation (20), which transcriptionally and translationally upregulates ER chaperone levels. To examine UPR activation in thyrocytes, we monitored steady-state protein levels of BiP, GRP94, and CRT, three ER chaperones known to be upregulated by ER stress (30). Indeed, by Western blotting, all three chaperones were induced at 1 day after CST treatment and remained elevated thereafter (Fig. 10). The levels of CNX, which is not disproportionately upregulated in response to Tg misfolding in thyrocytes (30), served as a useful loading control in these experiments (Fig. 10). This is not to suggest that, after CST treatment, only BiP/GRP94/PDI becomes engaged with Tg while the lectin-like chaperones remain idle. Indeed, when PC-Cl3 thyrocytes were treated with CST postpulse rather than

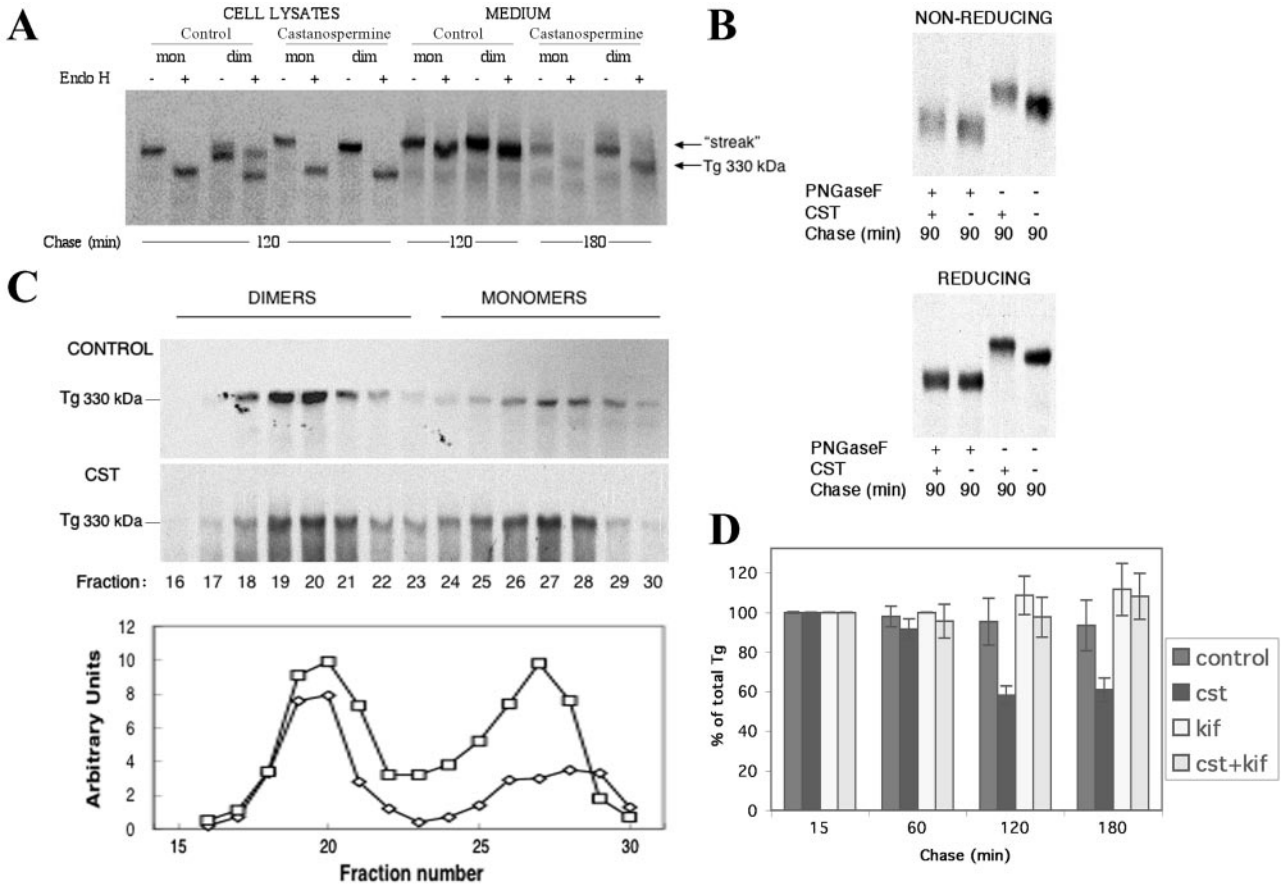

FIG. 8. CST inhibits efficient folding of Tg. (A) CST effect on oligosaccharide processing. PC-Cl3 cells were pretreated with CST, labeled, chased, and analyzed by sucrose gradient centrifugation exactly as described for Fig. 2B. Tg secreted to the media was also collected. All samples were immunoprecipitated for Tg and either mock-digested (−) or digested (+) with endo H. The samples were finally resolved by SDS-PAGE under reducing conditions. mon, monomer; dim, dimer. (B) CST inhibits oxidative folding. PC-Cl3 cells, pretreated (+) or not (−) with CST, were labeled as outlined in Materials and Methods and chased for 90 min. Cell lysates and culture media were immunoprecipitated with anti-Tg antibodies and mock digested (−) or digested (+) with PNGase F. Immunoprecipitates were analyzed by nonreducing and reducing SDS-PAGE as indicated and were run for an extra period of time for improved resolution. (C) CST inhibits dimerization. PC-Cl3 cells, pretreated or not with CST, were labeled as outlined in Materials and Methods and chased for 120 min. Equal fractions of cell lysates and medium were mixed to obtain total Tg for analysis by sucrose gradient centrifugation. The gradient fractions were immunoprecipitated with anti-Tg antibodies. The bottom panel provides arbitrary densitometry units for quantitation of the relative abundance of dimers versus monomers shown above. Squares, CST pretreatment; diamonds, control. (D) CST activates ERAD. PC-Cl3 cells pretreated for 1 h with no drugs (control), 1 mM CST, 100 μM kifunensine (kif), or 1 mM CST plus 100 μM kifunensine (cst + kif), were pulse-labeled and chased for the times indicated in the presence of these drugs. Newly synthesized Tg was recovered from cell lysates and culture media by immunoprecipitation and reducing SDS-PAGE, followed by quantitative densitometry of autoradiographs. Total Tg recovery (the sum of intracellular and secreted Tg) was quantified at each chase time, normalized to that recovered at the 15-min chase time.

before pulse-labeling (postpulse treatment causes prolongation of the monoglucosylated state of N-glycans on recently synthesized Tg), lectin-like chaperones in the ER became "locked on" to recently synthesized Tg, while BiP binding was essentially nil, and secretion of these molecules was blocked (Fig. 11). Nevertheless, as BiP interaction with misfolded ER lumenal proteins has been reported to be the proximal event specifically linked to the activation of UPR (5, 50), we are forced to conclude that misfolding of newly synthesized rather than previously synthesized Tg molecules in the ER was the primary initiator of UPR activation in these experiments.

DISCUSSION

Although there have been numerous descriptions of mixed disulfides between exportable proteins and ER resident proteins, until now, few if any of them (10, 34) satisfy the challenge put forth by Freedman to isolate mixed disulfides between endogenous oxidoreductases and endogenous unfolded secretory-protein substrates (17). In this study, we have provided the first description of ERp57-Tg and PDI-Tg conjugates. Tg is a very favorable substrate for such a study, as it is a highly expressed endogenous secretory protein that requires 60 to 90 min to complete formation of its 60 disulfide bonds (14). Tg strongly interacts with the lectin-like chaperones (14), especially CRT (Fig. 4B), that in turn facilitate association with the ERp57 oxidoreductase. Overall, dissociation of newly synthesized Tg from BiP and GRP94 occurs with kinetics that overlap with the dissociation of Tg from CRT/CNX (14, 26, 27, 31, 43). However, Tg is a protein with multiple repeat domains, and there is evidence to suggest that these modules form indepen-

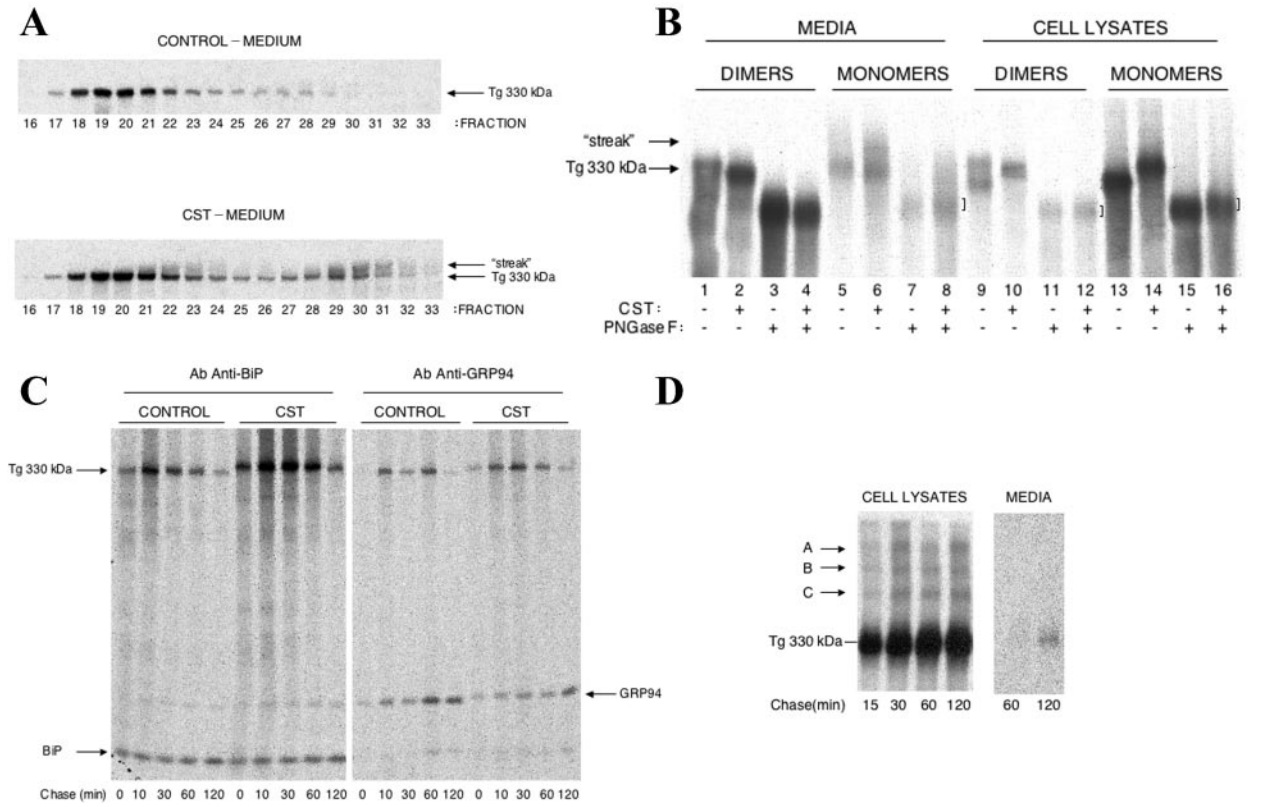

FIG. 9. CST compromises quality control, causing increased secretion of Tg monomers. (A) CST causes secretion of Tg monomers. PC-Cl3 cells, pretreated or not with CST, were labeled as outlined in Materials and Methods and chased for 120 min. Chase media were analyzed by sucrose sedimentation velocity centrifugation, and the gradients were collected beginning from the bottom of the tube. Each gradient fraction was immunoprecipitated with anti-Tg antibodies. The Tg dimer peak is to the left (lower fraction numbers), and the monomer peak is to the right (higher fraction numbers). (B) Tg monomers secreted following CST pretreatment are at least partially misfolded. PC-Cl3 cells, pretreated (+) or not (−) with CST, were labeled as outlined in Materials and Methods and chased for 90 min. Dimers and monomers from cell lysates and culture media were separated by sucrose velocity gradient centrifugation. Selected fractions from dimer and monomer peaks were immunoprecipitated with anti-Tg antibodies and mock digested (−) or digested (+) with PNGase F. Immunoprecipitates were analyzed by nonreducing SDS-PAGE run for an extra period of time for improved resolution. Brackets highlight a subtle distinction in the mobilities of partially oxidized Tg monomers and better-oxidized intracellular Tg dimers. (C) CST causes a dramatic increase of Tg binding to BiP and GRP94. PC-Cl3 cells, pretreated or not with CST, were labeled as outlined in Materials and Methods and chased for various times. Intact cells were cross-linked with DSP as outlined in Materials and Methods and lysed. Cell lysates were subjected to immunoprecipitation with anti-BiP and anti-GRP94 antibodies. Immunoprecipitates were resolved by reducing SDS-PAGE. The positions of Tg, BiP, and GRP94 are indicated. (D) Delayed maturation of disulfide-linked Tg adducts in cells treated with thapsigargin. PC-Cl3 cells were labeled as outlined in Materials and Methods and chased for the times indicated. Newly synthesized Tg was recovered by immunoprecipitation and SDS-PAGE under nonreducing conditions. The positions of the 330-kDa Tg and intermolecular disulfide-bonded complexes (A, B, and C) are indicated. The gels were intentionally overexposed for optimal detection of disulfide-linked Tg adducts.

dently folded units (14, 48). We presume that some of these domains prefer initial interaction with CRT/CNX, based on the fact that at least 6 of 16 cysteine-rich repeat modules contain N-linked glycosylation sites with experimentally proven N-glycans directly within the repeat (49), while other sites are more likely to favor BiP. Presumably, the formation of intradomain disulfide bonds is then catalyzed near CRT/CNX-bound sites by the ERp57 oxidoreductase and near BiP-bound sites by PDI. We do not yet know if the importance of these oxidoreductase activities is completely exclusive to initial modular intradomain folding or if subsequent three-dimensional interdomain packing of the monomeric polypeptide may also require the catalyzed formation of a few critical intrachain disulfide bridges.

By nonreducing SDS-PAGE, we found at least three high-molecular-mass bands that appear to represent disulfide-linked adducts of newly synthesized Tg (Fig. 1). None of the adducts reach the Golgi complex (Fig. 2), all of the adducts employ monomeric Tg, and all of the adducts are split into component parts under reducing conditions, showing that they are comprised directly of mixed disulfides between Tg and other proteins in the 50- to 80-kDa range (Fig. 4A). In this report, we have established that immunoprecipitation of ERp57 plus PDI can quantitatively precipitate Tg adduct "B," which appears to be comprised of two subcomponents (Fig. 4C). We have shown that this is not a coimmunoprecipitation but represents direct immunoprecipitation of covalently linked Tg-ERp57 and Tg-PDI adducts (Fig. 4D). Moreover, because ERp57 binding is already evident upon translation of only the amino-terminal portion of the Tg molecule (Fig. 6), this asso-

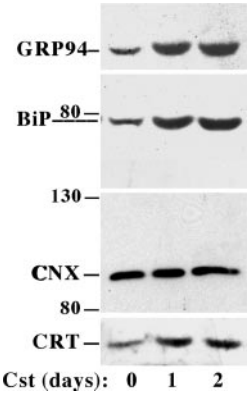

FIG. 10. CST treatment causes the upregulation of ER chaperone levels indicative of UPR activation. FRTL-5 cells growing in complete media were treated with 1 mM CST for the number of days indicated. Cells were lysed, and 25 μg of each lysate was analyzed by SDS-PAGE and Western blotting with each of the antibodies shown. The positions of selected molecular mass markers are indicated (in kilodaltons). CRT migrated as an ~58-kDa band. This experiment was repeated four times, revealing an approximately threefold increase in GRP94, BiP, and CRT after both 1 and 2 days of treatment.

ciation begins even before the full Tg polypeptide becomes available for folding in the ER lumen. Indeed, the adducts are most abundant at the earliest chase times, their mass is converted in a "precursor-product" relationship to monomeric Tg, and their disappearance is not prevented by inhibition of ERAD with either proteasome inhibitor or kifunensine (Fig. 3). Thus, although the data do not formally exclude the possibility of ERAD for some subpopulation of disulfide-linked Tg

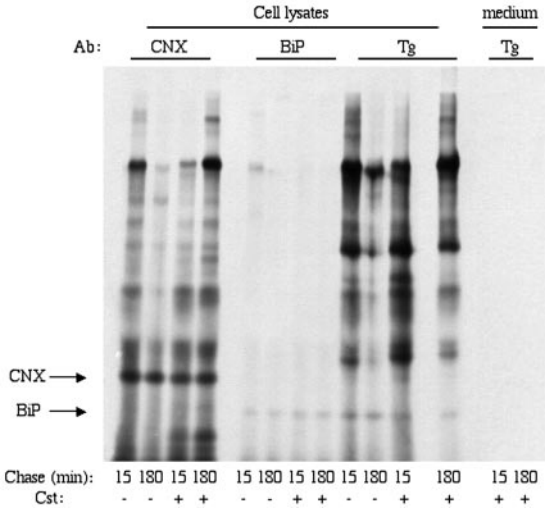

FIG. 11. Prevention of escape from the CRT/CNX cycle is also deleterious for labeled Tg progression through the secretory pathway. PC-Cl3 cells were not pretreated but labeled as outlined in Materials and Methods and then mock incubated (−) or incubated (+) in the presence of CST only during the chase periods shown. Cell lysates and culture media were immunoprecipitated with anti-CNX, anti-BiP, and anti-Tg antibodies (Ab) and resolved by nonreducing SDS-PAGE. Note that CST treatment postpulse caused intracellular Tg retention in association with CNX.

complexes, the data are consistent with the possibility that these adducts are "on pathway" in Tg folding.

Observed association of the CRT/CNX/ERp57 system, with the first N-linked glycosylation site at position 110 (that is conserved between species), is not necessarily consistent in detail with the hypothesis that preferential interaction with this system requires that the lectin-binding site appear within the first ~50 amino-terminal residues during growth of the nascent chain (41). Nevertheless, we are quite certain that the preferred ERp57 interaction is dependent upon the lectin-like activity of CRT/CNX, because the interaction is lost if the microsomes are pretreated with CST (Fig. 6). We note that ERp57 forms at least two distinct adduct bands with truncated Tg in vitro, while primarily only one adduct band is detected by immunoprecipitation from cells in vivo. More work is needed to identify which cysteine residues of Tg are attacked by ERp57, whether other ER oxidoreductases may covalently interact with the nascent Tg polypeptide, and whether the stoichiometry of oxidoreductases with the full-length Tg protein is always 1:1.

We could not obtain evidence for Tg progressing from one chaperone-oxidoreductase complex to another, although we prefer to not yet draw any firm conclusion from this observation. What is abundantly clear from the present results is that prevention of newly synthesized Tg association with the CRT/CNX/ERp57 system has several dramatic consequences. First, there was impairment/delay in oxidative folding of Tg monomers (Fig. 8B). Second, there was impairment/delay of Tg dimerization (Fig. 8C). Third, there was an increased fraction of newly synthesized Tg molecules subjected to ERAD (Fig. 8D). Consequently, there was diminished secretion of newly synthesized Tg (Fig. 7).

We were initially surprised that the extent of the diminution of secretion was less than one might expect (16), given the fact that BiP/PDI was relocated onto newly synthesized Tg (Fig. 5 and 9C) and other proteins to a level sufficient to activate the unfolded protein response (Fig. 10). At least a part of the explanation for the preservation of labeled Tg secretion under these circumstances is a loss of quality control such that Tg monomers were no longer efficiently retained within the ER (Fig. 9A). Many of these secreted monomers still had not completed the disulfide maturation process (Fig. 9B), and some of them had then undergone abnormal Golgi-based post-translational modifications consistent with surfaces of the Tg molecule being abnormally exposed to Golgi processing enzymes. These data point to the notion that CRT/CNX are important ER retention factors for improperly folded Tg conformers. In support of this view, when CST was added postpulse rather than in pretreatment, the CRT/CNX system was actively engaged and Tg was fully retained within the cells (Fig. 11).

Altogether, the data in this report lead us to suggest that the normal Tg folding pathway proceeds with the aid of at least two ER oxidoreductases, ERp57 (engaged with the CRT/CNX system) and PDI (likely to be engaged with the BiP system), forming direct mixed-disulfide adducts with newly synthesized Tg. We have no way of selectively disrupting Tg-PDI association in thyrocytes; however, when initial Tg-ERp57 association is prevented, multiple defects appear in the Tg secretory pathway, indicating that PDI cannot efficiently compensate for the absence of ERp57 function. Plausibly, such inability of PDI to

efficiently substitute for ERp57 could be explained if these chaperone-oxidoreductase complexes were located in physically distinct subregions of the ER (18, 24). However, such a concept will be difficult to reconcile if it can be proven that the same Tg monomers are simultaneously engaged with both chaperone-oxidoreductase systems and do not progress from one oxidoreductase complex to another (Fig. 5).

ACKNOWLEDGMENTS

This work was supported by FIRB grants no. RBNE0155LB-006 and PRIN 2004062075-004 of the MIUR (to B.D.J.) and from NIH DK40344 (to P.A.).

We also thank E. Consiglio and S. Formisano for support.

REFERENCES

1. **Anelli, T., M. Alessio, A. Bachi, L. Bergamelli, G. Bertoli, S. Camerini, A. Mezghrani, E. Ruffato, T. Simmen, and R. Sitia.** 2003. Thiol-mediated protein retention in the endoplasmic reticulum: the role of ERp44. EMBO J. **22:**5015–5022.
2. **Anelli, T., M. Alessio, A. Mezghrani, T. Simmen, F. Talamo, A. Bachi, and R. Sitia.** 2002. ERp44, a novel endoplasmic reticulum folding assistant of the thioredoxin family. EMBO J. **21:**835–844.
3. **Antoniou, A. N., S. Ford, M. Alphey, A. Osborne, T. Elliott, and S. J. Powis.** 2002. The oxidoreductase ERp57 efficiently reduces partially folded in preference to fully folded MHC class I molecules. EMBO J. **21:**2655–2663.
4. **Bergeron, J. J. M., M. B. Brenner, D. Y. Thomas, and D. B. Williams.** 1994. Calnexin: a membrane-bound chaperone of the endoplasmic reticulum. Trends Biochem. Sci. **19:**124–128.
5. **Bertolotti, A., Y. Zhang, L. M. Hendershot, H. P. Harding, and D. Ron.** 2000. Dynamic interaction of BiP and ER stress transducers in the unfolded-protein response. Nat. Cell Biol. **2:**326–332.
6. **Braakman, I., J. Helenius, and A. Helenius.** 1992. Manipulating disulfide bond formation and protein folding in the endoplasmic reticulum. EMBO J. **11:**1717–1722.
7. **Braakman, I., J. Helenius, and A. Helenius.** 1992. Role of ATP and disulphide bonds during protein folding in the endoplasmic reticulum. Nature (London) **356:**260–262.
8. **Brown, K., S. Park, T. Kanno, G. Franzoso, and U. Siebenlist.** 1993. Mutual regulation of the transcriptional activator NF-kappa B and its inhibitor, I kappa B-alpha. Proc. Natl. Acad. Sci. USA **90:**2532–2536.
9. **Chung, K. T., Y. Shen, and L. M. Hendershot.** 2002. BAP, a mammalian BiP-associated protein, is a nucleotide exchange factor that regulates the ATPase activity of BiP. J. Biol. Chem. **277:**47557–47563.
10. **Dick, T. P., N. Bangia, D. R. Peaper, and P. Cresswell.** 2002. Disulfide bond isomerization and the assembly of MHC class I-peptide complexes. Immunity **16:**87–98.
11. **Di Jeso, B., and P. Arvan.** 2004. Thyroglobulin structure, function, and biosynthesis, p. 77–95. *In* L. E. Braverman and R. Utiger (ed.), The thyroid, 9th ed. Lippincott Williams & Wilkins, Philadelphia, Pa.
12. **Di Jeso, B., D. Liguoro, P. Ferranti, et al.** 1992. Modulation of the carbohydrate moiety of thyroglobulin by thyrotropin and calcium in Fisher rat thyroid line-5 cells. J. Biol. Chem. **267:**1938–1944.
13. **Di Jeso, B., R. Pereira, E. Consiglio, S. Formisano, J. Satrustegui, and I. V. Sandoval.** 1998. Demonstration of a Ca^{2+} requirement for thyroglobulin dimerization and export to the Golgi complex. Eur. J. Biochem. **252:**583–590.
14. **Di Jeso, B., L. Ulianich, F. Pacifico, A. Leonardi, P. Vito, E. Consiglio, S. Formisano, and P. Arvan.** 2003. The folding of thyroglobulin in the calnexin/calreticulin pathway and its alteration by a loss of Ca^{2+} from the endoplasmic reticulum. Biochem. J. **370:**449–458.
15. **Elliott, J. G., J. D. Oliver, and S. High.** 1997. The thiol-dependent reductase ERp57 interacts specifically with *N*-glycosylated integral membrane proteins. J. Biol. Chem. **272:**13849–13855.
16. **Franc, J. L., A. Giraud, and J. Lanet.** 1990. Effects of deoxymannojirimycin and castanospermine on the polarized secretion of thyroglobulin. Endocrinology **126:**1464–1470.
17. **Freedman, R.** 1999. Linking catalysts to chemistry. Nature **402:**27–28.
18. **Frenkel, Z., M. Shenkman, M. Kondratyev, and G. Z. Lederkremer.** 2004. Separate roles and different routing of calnexin and ERp57 in endoplasmic reticulum quality control revealed by interactions with asialoglycoprotein receptor chains. Mol. Biol. Cell **15:**2133–2142.
19. **Graves, P. N., and T. F. Davies.** 1990. A second thyroglobulin messenger RNA species (rTg-2) in rat thyrocytes. Mol. Endocrinol. **4:**155–161.
20. **Harding, H. P., M. Calfon, F. Urano, I. Novoa, and D. Ron.** 2002. Transcriptional and translational control in the mammalian unfolded protein response. Annu. Rev. Cell Dev. Biol. **18:**575–599.
21. **Helenius, A., and M. Aebi.** 2004. Roles of N-linked glycans in the endoplasmic reticulum. Annu. Rev. Biochem. **73:**1019–1049.
22. **Hosokawa, N., L. O. Tremblay, Z. You, A. Herscovics, I. Wada, and K. Nagata.** 2003. Enhancement of endoplasmic reticulum (ER) degradation of misfolded null Hong Kong alpha1-antitrypsin by human ER mannosidase I. J. Biol. Chem. **278:**26287–26294.
23. **Huppa, J. B., and H. L. Ploegh.** 1998. The eS-Sence of -SH in the ER. Cell **92:**145–148.
24. **Kamhi-Nesher, S., M. Shenkman, S. Tolchinsky, S. V. Fromm, R. Ehrlich, and G. Z. Lederkremer.** 2001. A novel quality control compartment derived from the endoplasmic reticulum. Mol. Biol. Cell **12:**1711–1723.
25. **Kellokumpu, S., M. Suokas, L. Risteli, and R. Myllyla.** 1997. Protein disulfide isomerase and newly synthesized procollagen chains form higher-order structures in the lumen of the endoplasmic reticulum. J. Biol. Chem. **272:**2770–2777.
26. **Kim, P., D. Bole, and P. Arvan.** 1992. Transient aggregation of nascent thyroglobulin in the endoplasmic reticulum: relationship to the molecular chaperone, BiP. J. Cell Biol. **118:**541–549.
27. **Kim, P. S., and P. Arvan.** 1995. Calnexin and BiP act as sequential molecular chaperones during thyroglobulin folding in the endoplasmic reticulum. J. Cell Biol. **128:**29–38.
28. **Kim, P. S., and P. Arvan.** 1991. Folding and assembly of newly synthesized thyroglobulin occurs in a pre-Golgi compartment. J. Biol. Chem. **266:**12412–12418.
29. **Kim, P. S., and P. Arvan.** 1993. Hormonal regulation of thyroglobulin export from the endoplasmic reticulum of cultured thyrocytes. J. Biol. Chem. **268:**4873–4879.
30. **Kim, P. S., O.-Y. Kwon, and P. Arvan.** 1996. An endoplasmic reticulum storage disease causing congenital goiter with hypothyroidism. J. Cell Biol. **133:**517–527.
31. **Kuznetsov, G., L. B. Chen, and S. K. Nigam.** 1994. Several endoplasmic reticulum stress proteins, including ERp72, interact with thyroglobulin during its maturation. J. Biol. Chem. **269:**22990–22995.
32. **Leach, M. R., and D. B. Williams.** 2004. Lectin-deficient calnexin is capable of binding class I histocompatibility molecules in vivo and preventing their degradation. J. Biol. Chem. **279:**9072–9079.
33. **Leonardi, A., P. Vito, C. Mauro, F. Pacifico, L. Ulianich, E. Consiglio, S. Formisano, and B. Di Jeso.** 2002. Endoplasmic reticulum stress causes thyroglobulin retention in this organelle and triggers activation of nuclear factor-kappa B via tumor necrosis factor receptor-associated factor 2. Endocrinology **143:**2169–2177.
34. **Lindquist, J. A., G. J. Hammerling, and J. Trowsdale.** 2001. ER60/ERp57 forms disulfide-bonded intermediates with MHC class I heavy chain. FASEB J. **8:**1448–1450.
35. **Mast, S. W., K. Diekman, K. Karaveg, A. Davis, R. N. Sifers, and K. W. Moremen.** 2005. Human EDEM2, a novel homolog of family 47 glycosidases, is involved in ER-associated degradation of glycoproteins. Glycobiology **15:**421–436. [Online.]
36. **Mayer, M., U. Kies, R. Kammermeier, and J. Buchner.** 2000. BiP and PDI cooperate in the oxidative folding of antibodies in vitro. J. Biol. Chem. **275:**29421–29425.
37. **Meunier, L., Y. K. Usherwood, K. T. Chung, and L. M. Hendershot.** 2002. A subset of chaperones and folding enzymes form multiprotein complexes in endoplasmic reticulum to bind nascent proteins. Mol. Biol. Cell **13:**4456–4469.
38. **Mezghrani, A., A. Fassio, A. Benham, T. Simmen, I. Braakman, and R. Sitia.** 2001. Manipulation of oxidative protein folding and PDI redox state in mammalian cells. EMBO J. **20:**6288–6296.
39. **Molinari, M., V. Calanca, C. Galli, P. Lucca, and P. Paganetti.** 2003. Role of EDEM in the release of misfolded glycoproteins from the calnexin cycle. Science **299:**1397–1400.
40. **Molinari, M., K. K. Eriksson, V. Calanca, C. Galli, P. Cresswell, M. Michalak, and A. Helenius.** 2004. Contrasting functions of calreticulin and calnexin in glycoprotein folding and ER quality control. Mol. Cell **13:**125–135.
41. **Molinari, M., and A. Helenius.** 2000. Chaperone selection during glycoprotein translocation into the endoplasmic reticulum. Science **288:**331–333.
42. **Molinari, M., and A. Helenius.** 1999. Glycoproteins form mixed disulphides with oxidoreductases during folding in living cells. Nature **402:**90–93.
43. **Muresan, Z., and P. Arvan.** 1997. Thyroglobulin transport along the secretory pathway. Investigation of the role of molecular chaperone, GRP94, in protein export from the endoplasmic reticulum. J. Biol. Chem. **272:**26095–26102.
44. **Oda, Y., N. Hosokawa, I. Wada, and K. Nagata.** 2003. EDEM as an acceptor of terminally misfolded glycoproteins released from calnexin. Science **299:**1394–1397.
45. **Olivari, S., C. Galli, H. Alanen, L. Ruddock, and M. Molinari.** 2005. A novel stress-induced EDEM variant regulating endoplasmic reticulum-associated glycoprotein degradation. J. Biol. Chem. **280:**2424–2428.
46. **Oliver, J. D., H. L. Roderick, D. H. Llewellyn, and S. High.** 1999. ERp57 functions as a subunit of specific complexes formed with the ER lectins calreticulin and calnexin. Mol. Biol. Cell **10:**2573–2582.
47. **Oliver, J. D., F. J. van der Wal, N. J. Bulleid, and S. High.** 1997. Interaction of the thiol-dependent reductase ERp57 with nascent glycoproteins. Science **275:**86–88.
48. **Park, Y. N., and P. Arvan.** 2004. The acetylcholinesterase-homology region is essential for normal conformational maturation and secretion of thyroglobulin. J. Biol. Chem. **279:**17085–17089.

49. **Rawitch, A. B., H. G. Pollock, and S. X. Yang.** 1993. Thyroglobulin glycosylation: location and nature of the N-linked oligosaccharide units in bovine thyroglobulin. Arch. Biochem. Biophys. **300:**271–279.
50. **Shen, J., X. Chen, L. Hendershot, and R. Prywes.** 2002. ER stress regulation of ATF6 localization by dissociation of BiP/GRP78 binding and unmasking of Golgi localization signals. Dev. Cell **3:**99–111.
51. **Tatu, U., and A. Helenius.** 1997. Interactions between newly synthesized glycoproteins, calnexin and a network of resident chaperones in the endoplasmic reticulum. J. Cell Biol. **136:**555–565.
52. **Tokunaga, F., C. Brostrom, T. Koide, and P. Arvan.** 2000. ER-associated degradation of misfolded N-linked glycoproteins is suppressed upon inhibition of ER mannosidase I. J. Biol. Chem. **275:**40757–40764.
53. **Wu, Y., M. T. Swulius, K. W. Moremen, and R. N. Sifers.** 2003. Elucidation of the molecular logic by which misfolded alpha 1-antitrypsin is preferentially selected for degradation. Proc. Natl. Acad. Sci. USA **100:**8229–8234.
54. **Zapun, A., N. J. Darby, D. C. Tessier, M. Michalak, J. J. Bergeron, and D. Y. Thomas.** 1998. Enhanced catalysis of ribonuclease B folding by the interaction of calnexin or calreticulin with ERp57. J. Biol. Chem. **273:**6009–6012.